0273-2289/06/129–132/509–527/$30.00

Catalyst Transport in Corn Stover Internodes

Elucidating Transport Mechanisms Using Direct Blue-I

SRIDHAR VIAMAJALA,* MICHAEL J. SELIG, TODD B. VINZANT, MELVIN P. TUCKER, MICHAEL E. HIMMEL, JAMES D. MCMILLAN, AND STEPHEN R. DECKER

National Bioenergy Center, National Renewable Energy Laboratory, 1617 Cole Boulevard, Golden, CO 80401, E-mail: Sridhar_viamajala@nrel.gov

Abstract

The transport of catalysts (chemicals and enzymes) within plant biomass is believed to be a major bottleneck during thermochemical pretreatment and enzymatic conversion of lignocellulose. Subjecting biomass to size reduction and mechanical homogenization can reduce catalyst transport limitations; however, such processing adds complexity and cost to the overall process. Using high-resolution light microscopy, we have monitored the transport of an aqueous solution of Direct Blue-I (DB-I) dye through intact corn internodes under a variety of impregnation conditions. DB-I is a hydrophilic anionic dye with affinity for cellulose. This model system has enabled us to visualize likely barriers and mechanisms of catalyst transport in corn stems. Microscopic images were compared with calculated degrees of saturation (i.e., volume fraction of internode void space occupied by dye solution) to correlate impregnation strategies with dye distribution and transport mechanisms. Results show the waxy rind exterior and air trapped within individual cells to be the major barriers to dye transport, whereas the vascular bundles, apoplastic continuum (i.e., the intercellular void space at cell junctions), and fissures formed during the drying process provided the most utilized pathways for transport. Although representing only 20–30% of the internode volume, complete saturation of the apoplast and vascular bundles by fluid allowed dye contact with a majority of the cells in the internode interior.

Index Entries: Biomass conversion; internode transport; dilute acid pretreatment; direct blue-I; biomass recalcitrance.

Introduction

Conversion of biomass to ethanol involves mechanical and catalytic steps to disrupt the complex lignocellulosic structure, exposing polysaccharides that can then be hydrolyzed to fermentable sugars. Catalysts, such as dilute sulfuric acid are used to condition or "pretreat" biomass

*Author to whom all correspondence and reprint requests should be addressed.

to increase its susceptibility to enzymatic hydrolysis (1,2). Uneven distribution of catalyst within the biomass tissue results in heterogeneous pretreatment zones, with only a fraction of the biomass exposed to optimal conditions (3). This situation can be especially problematic with dilute acid catalysis, as areas of excessive pretreatment lead to the formation of byproducts, such as furfural, which inhibit fermentation of downstream sugars and decrease conversion yields (2), whereas incomplete pretreatment zones result in lowered enzymatic digestibility (4).

Within the pulp and paper industries, efficient transport of catalyst into biomass has long been recognized as an important step in the pulping process. Unit operations to uniformly impregnate wood chips are often part of the process design and operation (5). In the biomass-to-ethanol process literature, the effects of catalyst transport have generally been neglected, although this issue has been recognized as one of the factors that could contribute to a decrease in xylan hydrolysis rates during dilute acid pretreatments (6). The lack of concern toward catalyst transport mechanisms results from several contributing factors, including the tendency to use milled biomass in batch laboratory experiments (6–8) and the use of compression screw feeders in larger scale studies, which exert high shear and cause biomass size reduction; examples are the Sunds reactor (9) or the StakeTech reactor (4). However, size reduction, either as a standalone unit operation or in a compression screw feeder system, can lead to significant increases in equipment and operating costs (2,10). In some cases, compression of the feed stock may in fact be detrimental to pretreatment, causing biomass pore structure collapse and leading to uneven heat and mass transfer during pretreatment (11). In an effort to understand the effect of catalyst impregnation on biomass conversion in this study, several methods of impregnation were employed, including soaking at various standard temperatures and atmospheric pressure, soaking under vacuum, and preheating of biomass in air before submersion. It was conceived that this latter approach would mimic the steam preheating, common in the pulping industry, and allow catalyst penetration as the hot entrained air contracted after submersion.

Corn stover is available in significant quantities for conversion to ethanol and other bio-based products (9). Corn stover included the leaves, sheaths, stalks, cobs, and husks, with stalks contributing to about 60% of the dry mass and at least 50% of the total stover carbohydrate (1). As shown in Fig. 1, the stalks consist of internodes and nodes, with internodes containing two-thirds of the total stalk dry- and carbohydrate-mass (1).

A typical internode cross-section depicts several morphologically and functionally different cell types (Fig. 1) with the dominant structures being pith, vascular bundles, and rind. The pith, characterized by relatively large, thin-walled parenchyma cells, comprises a volumetrically large portion of the internode. Parenchyma cells, with a thin primary cell wall and a *de minimus* secondary cell wall, function primarily as storage reservoirs in the

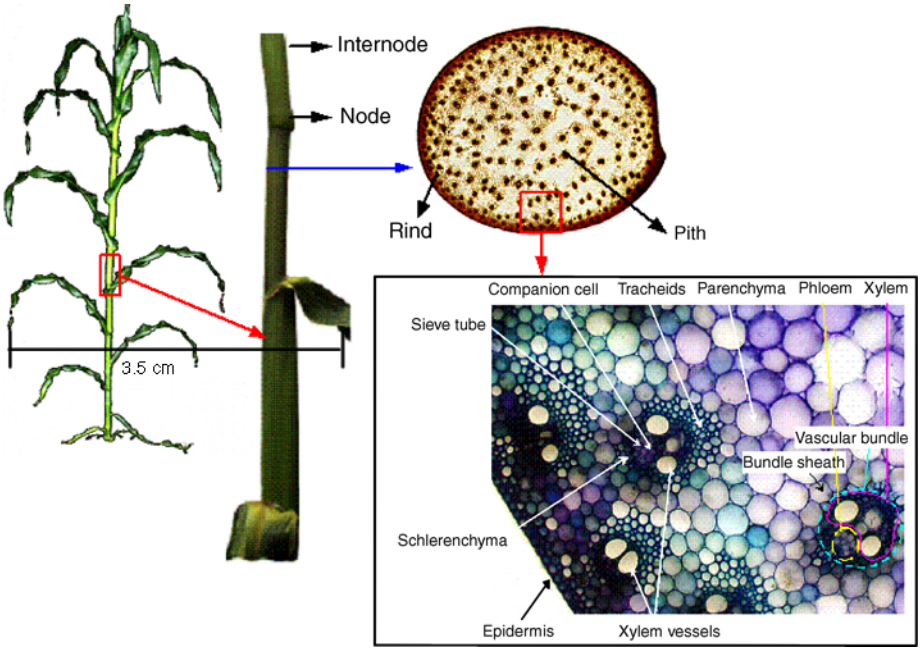

Fig. 1. Corn stover stem anatomy; adapted from Thomas et al. *(1)*, with permission.

internode. Although comprising a very large volumetric percentage of the plant, they included only about 11–12% of the mass in the internode *(12)*.

Distributed throughout the pith are vascular bundles, which run along the length of the corn stem. Mature vascular bundles are made up of an array of vascular tissues, primarily xylem, and phloem. The majority of the mass is sclerenchyma-derived xylem vessels and xylem tracheid fibers containing thick secondary cell walls. In the living plant these bundles serve as a means to transport water and nutrients along the length of the plant stem and leaves. Despite their relatively low contribution to the cross-sectional volume, the thick secondary cell walls of the vascular bundles increase their relative density, allowing the pith vascular bundles to make up approx 11–12% of the internode mass, about the same mass as the more volumetrically abundant parenchyma cells *(12)*.

The rind as a tissue type makes up about 75% of the mass of the internode and thus is a critical component for biomass conversion *(12)*. The rind layer has dense vascular bundles as well as collenchyma, parenchyma, and epidermal cells and is coated by an exterior waxy cuticle. The collenchyma cells are distinct from parenchyma in having thickened primary cell walls. The dense and water resistant nature of this protective layer can pose a significant barrier to catalyst transport.

Transport among nonvascular cells in a living plant is carried out through pits, areas of thin primary cell wall devoid of secondary cell wall among adjacent cells. Pits contain plasmodesmata, which are direct cytoplasmic connections among living cells. Pits also facilitate movement

of intracellular components between vascular cells and surrounding tissues. This plant-wide contiguous cytoplasm is referred to as the symplast. In contrast to the intracellular symplast, the apoplast is the intercellular space exterior to the cell membranes, providing a route for transport throughout the plant outside of the symplast (13). In dry senesced plants, the vascular bundles, pits, and apoplast may serve as conduits for catalyst transport.

Understanding how plant structure affects catalyst transport is a key to overcoming a number of pretreatment performance barriers traditionally addressed through costly process modifications. In this study, we have attempted to characterize the bulk transport characteristics of catalyst through dry intact corn stover using solutions of direct blue-I (DB-I) dye to simulate generic catalyst behavior. The affinity of DB-I for cellulose may mimic the binding of catalytic enzymes to cellulose; however, we are making no attempt to qualify or quantify this phenomenon. It should also be noted that the molecular weight of DB-I is about 10 times that of H_2SO_4, placing limitations on the routes of penetration used by DB-I in comparison with H_2SO_4. These differences, however, are likely to be undetectable as both limits are far below the resolving capacity of light microscopy. Using corn stem internodes to provide a simplified and reproducible model system, we have observed dye transport over a range of impregnation conditions. Through light microscopy and subsequent image analysis, we have observed in the internode matrix, a number of possible catalyst transport barriers and pathways.

Methods

Corn Stover

Whole corn stover, hand-cut from a single field at the Gustafson Farm in Weld County, CO, was derived from Round-Up Ready Pioneer corn hybrid, 36N18. The plants, cut in mid-January of 2005, had completely senesced in the field. At cutting, the average moisture content of the corn stalks was roughly 20%, which was reduced by air-drying to about 10% moisture content before any further preparations. For this study, the third, fourth, and fifth internodes from the base of the corn stalk were cut from the dried stalks using a size 3/0 jeweler's saw blade. All nodes were removed to provide a relatively uniform structure from which smaller segments could be cut.

Measurement of Internode Densities and Void Fraction

The bulk density (ρ_{bulk}), tissue density (ρ_{abs}), and void fraction (ε) were calculated for the internodes used in this study. This information was used to estimate the degree of impregnation (% saturation of the internode void space) that occurred during each impregnation scenario. Analysis of the saturation data was conducted in conjunction with microscopic inspection of the dye internodes in order to understand how the distribution

of catalyst (dye) throughout the internode correlated with the degree of impregnation under different conditions. For this study, bulk density is defined as the ratio of the internode mass to the volume of the intact structure. Saturation is defined as the potential amount of dye that can fill all spaces in the biomass, both empty air spaces inside cells and vessels, as well as any gaps between cell wall components. It is estimated from the experimentally determined difference in bulk densities of intact and finely milled internodes. The volume, in this case, is the sum of the volume of the plant tissue and the air trapped within the internode. The absolute density is defined as the average density of the solid tissue alone.

To measure average bulk density, approx 60 internode segments, each 3–5 cm in length, were cut from larger internode sections. The air-dried mass of each segment was recorded to the nearest 0.1 mg. Segment volume was measured to the nearest 0.1 mL by volumetric displacement and then corrected for any water absorption that occurred during the measurements by differential mass measurements. Segments were then oven dried at 105°C overnight in order to obtain a dry mass value. The average internode bulk density was then calculated (m/V) on the basis of both the air-dried and oven-dried masses.

Absolute density was measured by milling a number of internodes to pass a 20-mesh screen. A known amount of water was added to a measured mass of milled stover, vortexed briefly, and centrifuged for 10 min at 1500*g*. After centrifugation, the difference between the total volume and the liquid volume was taken as the solids volume and used to calculate ρ_{abs}. Using both the absolute and bulk densities, the average internode void fraction (Eq. 1) was calculated.

$$\text{Void Fraction} = \varepsilon = 1 - (\rho_{bulk}/\rho_{abs}) \quad (1)$$

Transport Studies With DB-I

Powdered DB-I was obtained from Pylam Products Company Inc., Tempe, Arizona. In general, direct dyes are anionic and have a planar aromatic structure and a strong affinity for cellulose. DB-I, often referred to as pontamine sky blue, is a tetrasulfonated dye with a molecular weight of 993 and a molecular diameter of about 1 nm. Solutions of 1% and 0.5% (w/v) were prepared in water from the powdered dye for use throughout this study *(14)*.

Preparation of Internodes

Segments measuring 3.5 cm ± 0.1 cm in length, were cut from the larger internode sections and the ends were briefly exposed to moderate vacuum (approx 10 inch Hg) in order to remove debris from the cutting process that may have been lodged in any open-ended structures, such as the vascular bundles. The air-dried mass (m_{dry}) of each internode segment was recorded to the nearest 0.1 mg. The internode volume (V_{tot}) and void

volume (V_{void}) were approximated for each segment using the following equations:

$$V_{tot} = m_{dry}/\rho_{bulk} \quad (2)$$

$$V_{void} = V_{tot}\varepsilon \quad (3)$$

Impregnation of Internode Segments With DB-I

Dye transport through internode sections was studied under three impregnation conditions:

1. submersion in dye solution at atmospheric pressure and varying temperatures,
2. submersion under varying vacuum pressure, and
3. preheating segments in air before submersion into room temperature dye solution.

At atmospheric pressure, segments were impregnated at room temperature (approx 22°C) for a range of exposure times between 10 s and 24 h. Segments were also impregnated at atmospheric pressure with dye solutions heated to 50, 60, 70, 80, and 90°C over a range of exposure times between 30 s and 2 h. To explore the effect of vacuum pressure, segments were impregnated under a 22.5 inch Hg vacuum for exposure times between 30 s and 24 h. In addition, the effect of lower vacuum pressures (5, 10, 15, and 20 inch Hg) was also tested for shorter exposure times (1–30 min). The effect of preheating on impregnation was studied by heating segments in an oven that was set to the desired temperature. After fixed exposure times, the hot segments were rapidly transferred into room temperature dye solution and submerged for 5 min. In this study, segments were oven heated for 5, 10, and 20 min at the following temperatures: 50, 60, 85, 105, and 120°C.

For all impregnations, internode segments were completely submerged in DB-I solution and either held stationary with metal tongs for short duration exposures or weighed down with stainless steel hose clamps for long-term exposures. Triplicate segments were dyed for all time points under all conditions. On removal from the dye solution, any excess dye was wiped from the exterior of each segment and the mass was recorded to the nearest 0.1 mg. This "wet" mass was then used to calculate an approximate value for the percent saturation (Eq. 4) of the segments void space.

$$\%\ \text{Saturation} = 100*((m_{wet} - m_{dry})/\rho_{dye})/(V_{void}) \quad (4)$$

Microscopy: Sectioning and Image Analysis

After impregnation, internode segments were air-dried in a laminar flow hood before any manipulation. Dry segments were laterally bisected by hand using Performa Super double-edged razor blades from the

Table 1
Corn Stover Density Measurements From Literature

Authors	Bulk density (g/cm^3)	Tissue density (g/cm^3)
This study	0.13	1.13
Mani et al. *(15)* Set 1	0.132	1.14
Mani et al. *(15)* Set 2	0.156	1.171
Mani et al. *(15)* Set 3	0.158	1.179
Thomas et al. *(1)* Set 1	0.11	NA
Thomas et al. *(1)* Set 2	0.15	NA

American Safety Razor Company in Verona, VA. In order to evaluate dye movement along the length of the internode, images of the internal face of the bisected segments were captured using a Zeiss Stemi 2000-C stereomicroscope. The microscope was attached with a Sony DSP 3 CCD color video camera. A few wet segments were laterally bisected to check for dye movement that may have occurred during drying. After stereomicroscope imaging, lateral and transverse thin sections (approx 0.5 mm) were cut from the bisected halves. Before making transverse sections, the rind was removed to facilitate easy and uniform thickness cuts. Thin sections were imaged using an Olympus DP70 Microscope Digital Camera (maximum resolution of approx 12.5 million pixels) attached to an Olympus IX71 Inverted Microscope.

Results

Internode Bulk Properties

The average bulk density was measured on the basis of both air-dried and oven-dried internodes. The average moisture content of the air-dried internodes was measured to be 9.3 ± 0.7% (N = 56). The average bulk density of air-dried internodes was measured to be 0.130 ± 0.007 g/cm^3 (N = 56) and the average bulk density of the internodes on an oven-dried basis (0% moisture) was 0.142 ± 0.009 g/cm^3 (N = 56). The air-dried bulk density was used for the remainder of the calculations in this study. The average absolute internode tissue density (air-dried basis) was determined to be 1.13 ± 0.05 g/cm^3 (N = 8). These measured corn stover densities were in agreement with previous measurements reported by Mani et al *(15)* and Thomas et al. *(1)* (Table 1).

Using the values for bulk density and absolute density, the void fraction of the air-dried internodes was estimated to be 0.89 ± 0.01. This void fraction was used to estimate the void volume of an internode segment (Eq. 3), which represents the volume of an air-dried internode that can be occupied by a catalyst solution. The void volume was further used to calculate the degree of saturation (Eq. 4) after impregnation, to provide an estimate of the volume occupied by dye solution as a fraction of the total

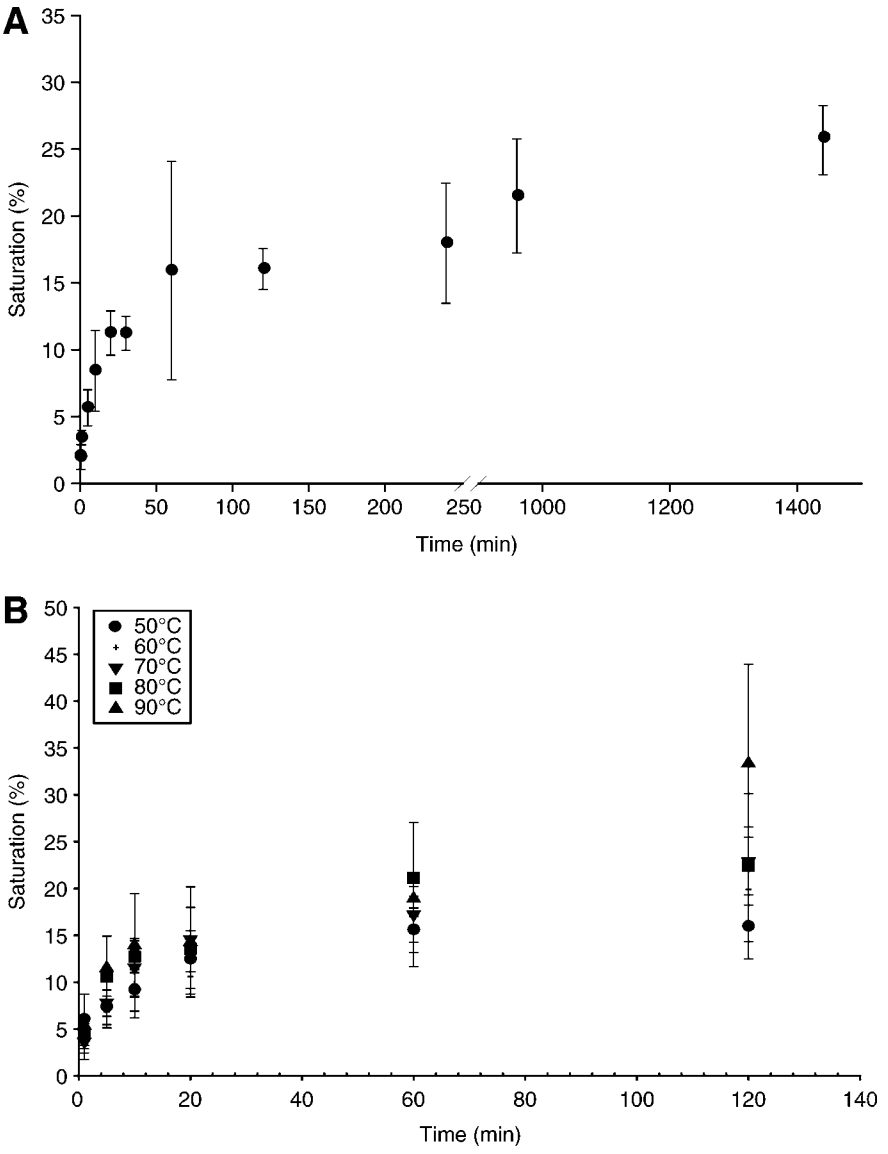

Fig. 2. Saturation of internode void space vs time after submerging in DB-I solution under atmospheric pressure at **(A)** room temperature and **(B)** varying dye temperatures.

available volume. This calculated degree of saturation was used to compare uptake of dye solution under the tested conditions.

Effect of Temperature and Pressure on Dye Uptake and Distribution

Impregnation at Atmospheric Pressure

Dye impregnation was very slow at room temperature and atmospheric pressure. Even after 24 h submerged in dye solution, a saturation of only 20–25% was achieved (Fig. 2A). When the segments were laterally

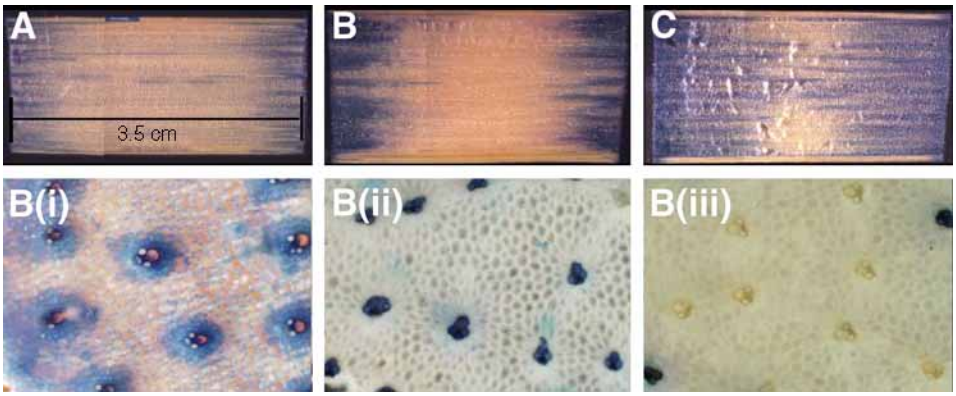

Fig. 3. Internode segments impregnated with DB-I at room temperature and atmospheric pressure. **(A)** lateral section after 5 min, **(B)** lateral section after 2 h; (i) 1 mm, (ii) 10 mm, and (iii) approx 175 mm from end; **(C)** lateral section after 24 h.

Fig. 4. Lateral sections of internodes impregnated with DB-I at atmospheric pressure and elevated temperatures: **(A)** 50°C for 2 h, **(B)** 70°C for 2 h, and **(C)** 90°C for 2 h.

bisected, dye movement was observed only along the length (Fig. 3) indicating that dye entered laterally through segment ends and not through the rind. After 24 h, although dye penetrated throughout the length of the piece, there were zones along the rind in which dye did not appear to reach. Increasing the temperature of the dye solution did not significantly improve dye uptake into the internodes. After 2 h of exposure to dye solution at higher temperatures, the saturation was only approx 25% and dye movement was restricted to internode ends. (Figs. 2B and 4). As can be seen in Fig. 4, the lateral dye movement profiles of internodes that were impregnated for 2 h were very similar throughout the entire temperature range. After 2 h of impregnation, dye was present both in the vascular bundles and the apoplast in sections 2 mm from the end. However, in sections that were 1 cm away from the end, dye was present only in the vascular bundles, whereas cross-sections cut through the middle of the internodes did not show any dye.

Vacuum Impregnation

Saturation of 25–40% of the void space was achieved immediately (<30 s) when segments were impregnated under 22.5 inch Hg vacuum (Fig. 5A). Under this condition, dye moved throughout the entire internode

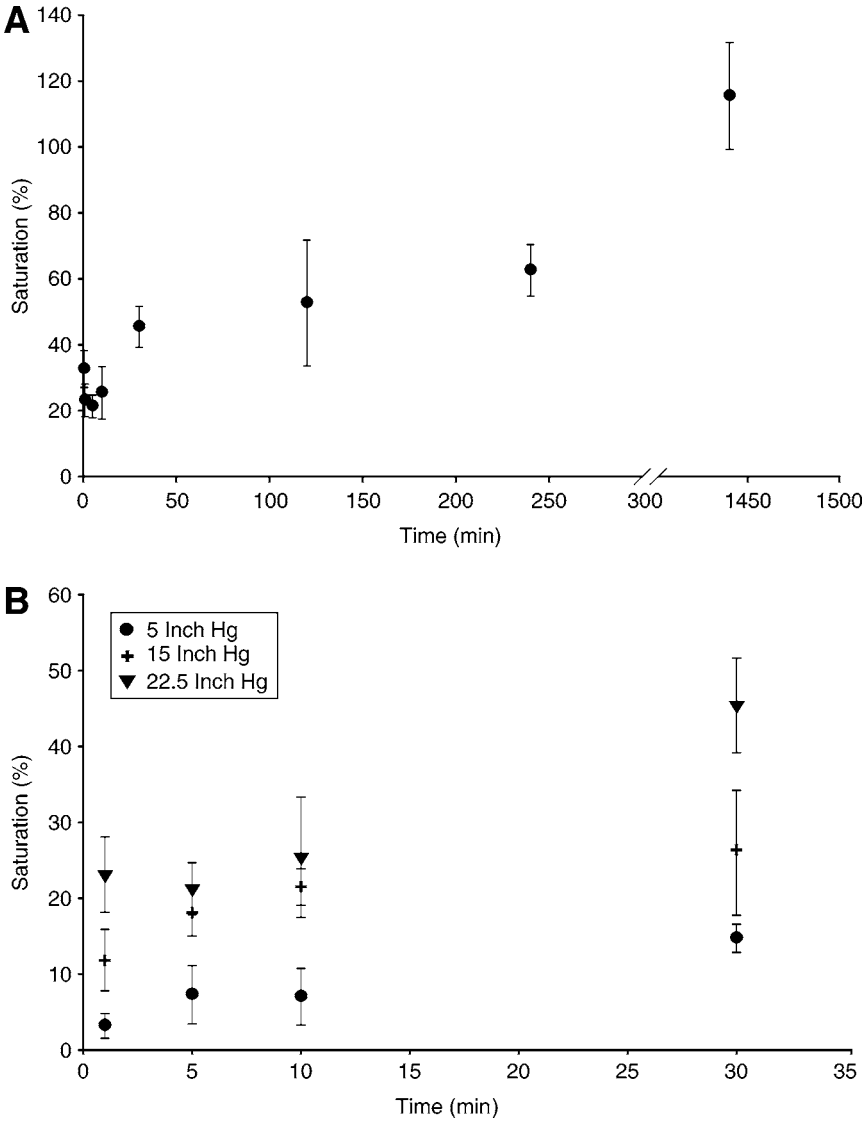

Fig. 5. Vacuum saturation of the internode void space after impregnation by submerging in DB-I under **(A)** 22.5 inch Hg and **(B)** varying vacuum pressures.

length and microscopic observation of cross-sections showed the presence of dye within and along the vascular bundles, as well as throughout the entire apoplastic continuum (Fig. 6). After the initial rapid saturation, further increase in moisture content in the internodes occurred at a much slower rate, and a long period under vacuum was required (>12 h) to achieve 100% saturation. At lower vacuum strengths, more time was required to achieve greater than 25% saturation (Fig. 5B). In cases in which internodes were less than 25% saturated, uniform dye distribution was not achieved (data not shown).

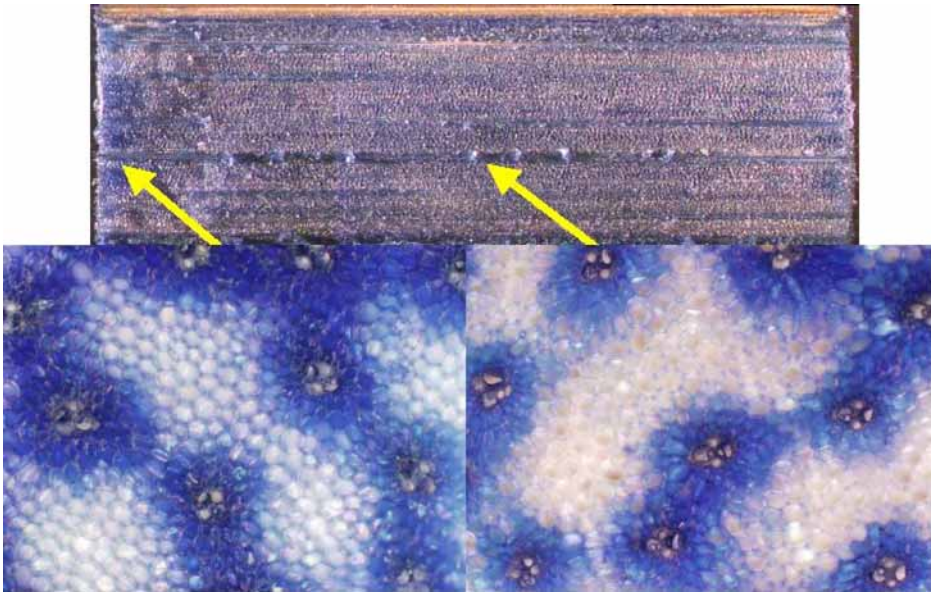

Fig. 6. Impregnating for 30 s under 22.5 inch Hg vacuum allowed for 30% saturation of the available void space. The lateral section shows uniform distribution of dye over the length of the internode whereas transverse sections at the ends (left) and the interior (right) show dye movement into the vascular bundle–parenchyma cell interface area.

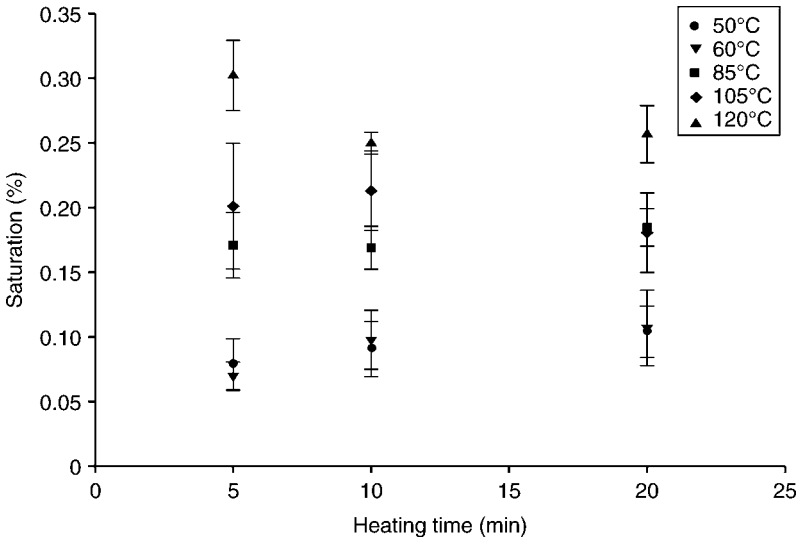

Fig. 7. Saturation of internode void space after preheating internodes segments and submerging in room temperature DB-I solution.

Dry Heat Impregnation of Internodes

Preheating dry internodes and then rapidly submerging them in dye solution was studied as another method of dye transport into internodes. As can be seen from Fig. 7, saturations levels of 20–30% could be achieved

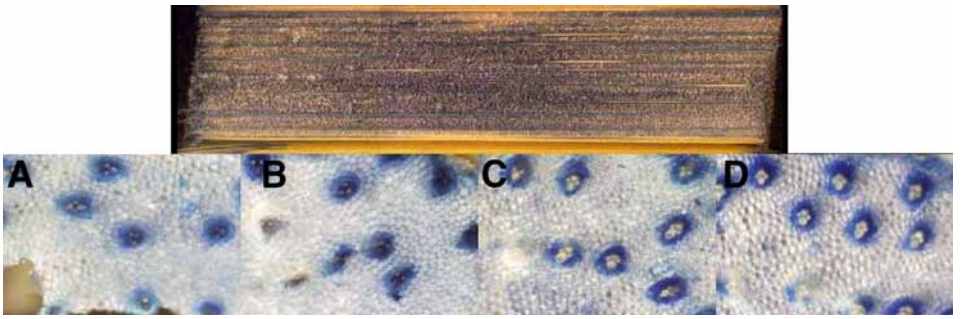

Fig. 8. Lateral and transverse sections of an internode preheated at 120°C for 15 min before submersion in DB-I solution. Cross-sections were taken from **(A)** 2 mm from left end, **(B)** 10 mm from left end, **(C)** at the internode midpoint, and **(D)** 5 mm from the right end.

by preheating pieces above 100°C for only 5 min and longer heating times did not appear to significantly enhance dye uptake (Fig. 7). Examination of lateral sections showed dye movement throughout the internode length at these saturation levels (Fig. 8). Closer examination of cross-sections showed that dye was present in most of the apoplastic space. Although dye was present both within and around the vascular bundles near the ends, it was present only in the apoplast around the vascular bundles in the center of the pieces, approx 175 mm from the cut end.

Discussion

Our experiments with DB-I revealed a number of pathways and barriers to the transport of dye into the model corn internode system. In general, the primary entry points were at the internode ends. Dye movement from this point occurred via four main pathways:

1. through the intercellular space surrounding parenchyma cells (the apoplastic continuum),
2. through vascular bundles,
3. along the parenchyma-vascular bundle interface, and
4. along the inner rind–pith interface.

Radial movement of dye into the internode through the rind was not observed, suggesting that the waxy outer surface of the rind acts as a barrier to penetration (just as nature intended). The mechanisms driving fluid into these pathways in dry corn stems are most likely to be capillary action, varying pressure differentials or a combination of both. The primary barriers to dye movement were the waxy outer surface of the rind and the air trapped within individual cells.

Pathways of Catalyst Distribution

The apoplastic continuum and vascular bundles are the major routes for dye transport into the internode. Whereas movement through the

vascular bundles is not surprising, because they form hollow channels in senesced plants, the extent and rapidity of liquid transport through the parenchymal apoplastic space was not anticipated. Although transport of dye through vascular bundles is obvious, it appears to be limited in extent compared to transport through the apoplast. Dye penetration through the vascular bundles under atmospheric conditions does not completely penetrate the entire bundle, presumably owing to the inability to displace the entrained air and through restriction by cellular junctions, perforation plates, and sieve plates.

Apoplast

Virtually all dye transport through the volumetric space occupied by thin-walled parenchyma tissue occurred via the intercellular space among cells, referred to here as the apoplastic continuum. The bulk of movement through this space presumably occurs at the junctures in which three or more cells come together and small air channels form during senescence. Although small, there appear to be several key factors that enhance the apoplast's role in catalyst distribution. First, the pathways with the apoplastic space are continuous and unimpeded. Unlike the vascular bundle components, in which transport is impeded by cell junctions, sieve plates, and perforation plates, the apoplastic continuum's main limitation is its narrow size. Second, the air passages within the apoplast, allow direct access of the catalyst to cell wall material, without the need to fill up the entire cell volume or to penetrate any residual membrane material. Examination of high magnification (×200) images (Fig. 9A,B) reveals clear ovular shaped disks formed by the abutment of cell walls from two adjacent parenchyma cells. From these images it was unclear whether or not dye penetrates into the middle lamella. How rapidly and extensively catalysts, specifically the hydronium ion and enzymes, can penetrate radially from the apoplastic continuum through the middle lamella and into the innermost layer of cell wall is still unanswered.

Because enzymes have specific affinities for biomass, much like the affinity of DB-I for cellulose, the potential exists for a titration effect of catalyst transported by the apoplast. We see indirect evidence of this in the fading of dye levels in parenchyma cells as you move radially out from the vascular bundles, but we do not have any direct evidence to support this idea. Images in Fig. 10 display distinct layers of cells surrounding the vascular bundles in which the cells walls appear to be dyed in decreasing hues of blue as they move outward. In these cases only a distinct layer of cells have their walls dyed blue. It is possible that high pressure differentials could drive the dye solution from the interior of vascular cells through pits and plasmodesmata and into adjacent parenchyma cells. The pressure differential would decrease as fluid moved into each subsequent layer of cells until it was not strong enough to push dye through into the next layer, and movement would essentially

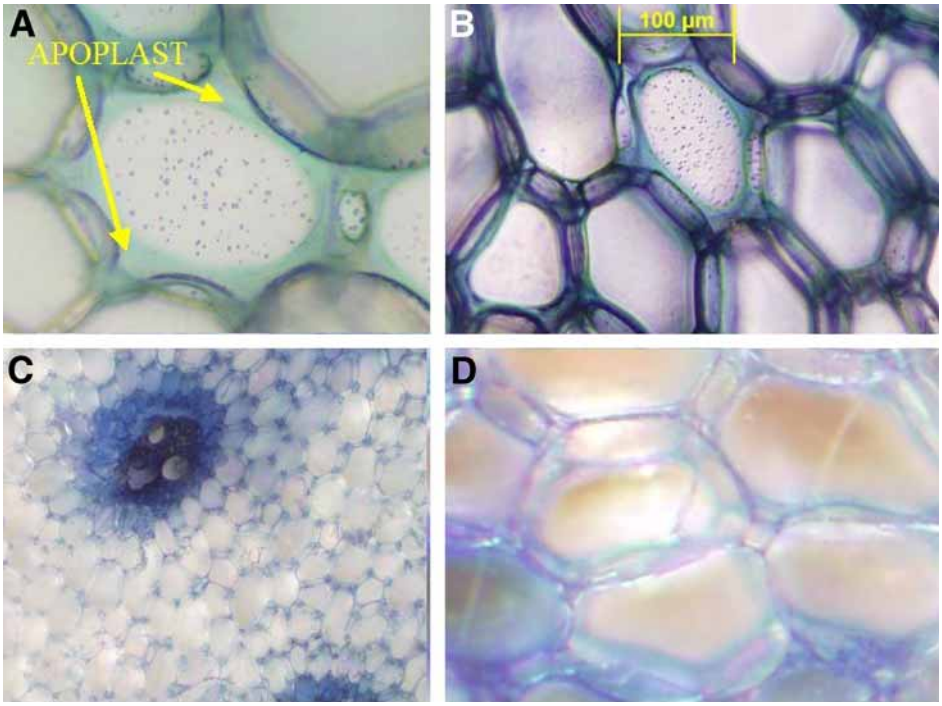

Fig. 9. Images showing dye movement through the intracellular spaces between parenchyma cells. Pits, cell wall junctions, and the apoplastic continuum framework are clearly visible in images taken at ×200 **(A,B)** with peripheral light source and at ×40 **(C)** and ×40 plus digital zooming **(D)** without peripheral light illumination.

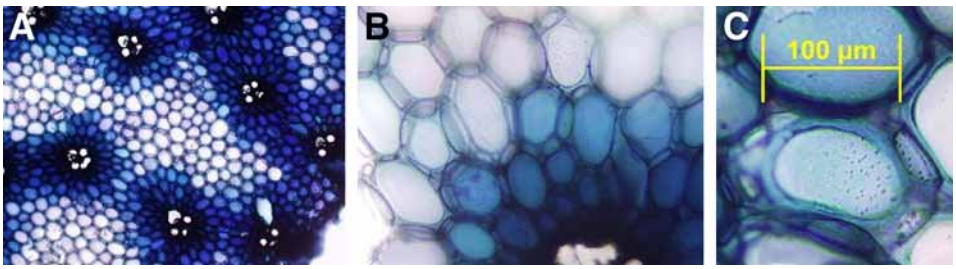

Fig. 10. Images of distinct layers of dyed cells surrounding the vascular bundles showing fading parenchymal dye levels distal to the vascular bundles. **A**, **B**, and **C** show increasing detail with higher magnification.

stop. More experimentation will be necessary to test this hypothesis through higher resolution, microscopy techniques.

Vascular Bundles

Vascular bundles provide the primary bulk fluid transport in living plants. These vessels provide convenient channels in dried biomass, but are limited in their ability to distribute catalyst radially into the parenchyma cells under any condition (*see* Fig. 10) and even laterally under

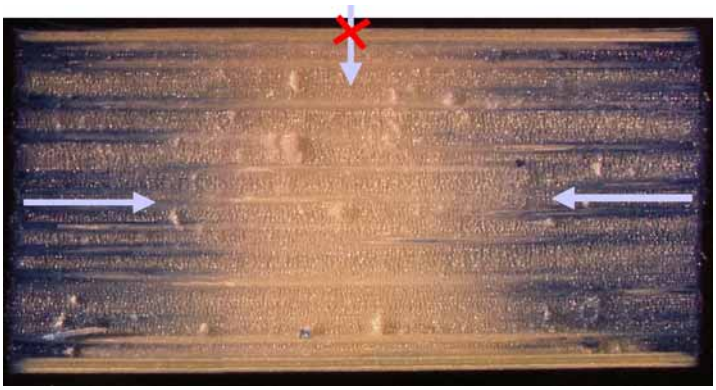

Fig. 11. Lateral cross-section of a dyed internode depicting dye movement from the cut ends of the internode into the interior and no movement through the exterior.

atmospheric pressure impregnation conditions (Fig. 3Biii). When impregnated under vacuum, the extent of transport in the vascular bundles is much greater, suggesting that the requirement for air displacement is a limitation (Fig. 6). When heating and submersion was used to impregnate the biomass, the vascular bundles did not show the same extent of interior transport as when vacuum was applied, however, the area immediately adjacent to the bundles was extensively saturated with dye (Fig. 8).

Vascular Bundle–Parenchyma Cell and Rind–Pith Interfaces

The vascular bundle–parenchyma cell interface, the result of differential shrinkage of the two tissue types during drying, appears to rapidly and extensively move dye the length of the internode. This transport route has the additional benefit of allowing direct access of catalyst to the apoplastic continuum along the length of the internode, without the need to penetrate the cell walls of vascular bundle cells. Presumably, a similar transport mechanism exists along the rind–pith interface. Dye movement in the vicinity of the rind was readily observed along the inner surface of the rind, through what we hypothesized to be cracks and fissures at the rind–parechyma interface. In some cases, this movement allowed for dye contact with the entire inner surface of the rind. Dye movement was also observed through the rind vascular bundles in a number of cases; however, the exterior of the rind completely blocked any movement of dye through the rind to the interior internode (Fig. 11). In all cases, dye transport occurred through the open ends of the internode. Because of this fact, it is probable that impregnation would be difficult with the scenario of a whole internode-node system in which the internode ends are not exposed. This observation indicates that at least a small degree of mechanical crushing or size reduction of corn stems is necessary to allow access of catalyst to the parenchyma though the cracks in the rind, as well as by creating cracks in the parenchyma. However, excessive mechanical shear and crushing could lead to collapse of the pore structure and result in poor catalyst penetration *(11)*.

Impregnation Barriers

Entrained Air

Although apoplastic movement of minerals is common in plants tissues, the air-trapped within parenchyma cells appears to be difficult to displace. The slow and incomplete movement of dye into the parenchyma cells under atmospheric pressure is likely owing to slow removal of the air trapped within cells. Under vacuum, this entrained air is removable, allowing for displacement by liquid. When the air is blocked from exiting however, such as by submersion in liquid, movement of liquid into the parenchyma intracellular space is prevented and movement in the apoplastic continuum is limited. The primary escape route for the entrapped air is likely through the plasmodesmata in pit fields that connect parenchyma cells. However, these pits are very small (approx 20 nm) and likely blocked owing to cell wall drying (data not shown). Note that the surface tension of water would prevent movement through these narrow pores into a dry space, especially if air displacement were limited. From these images it is unclear whether any dye actually penetrates into the cell wall beyond the apoplastic air gap. The air trapped within individual cells appears to be a primary barrier to dye movement through the internode.

Although Kim and Lee *(16)* have previously proposed diffusion into lignocellulosic biomass as the mass transfer mechanism, their experiments were performed with milled corn stover with a maximum particle size of 14 mesh. It is likely that at such small particle sizes, the cell structure is destroyed or disrupted and air contained within cells provides little if any barrier to being displaced by liquid. Whereas particle size reduction could result in rapid acid movement and contact with biomass *(16)*, milling biomass to a fine size is impractical on a large scale owing to the high-energy input required *(2)*. We hypothesized that heating intact internode sections would cause the entrained air to expand and on cooling by submersion in dye, the contracting air would be displaced by dye. This appeared to be the case, as heated samples rapidly took up dye on submersion and the dye distribution appeared to be rapid and extensive throughout the apoplast. Air removal techniques, such as vacuum or heat displacement of intracellular air, resulted in significantly improved dye penetration compared to diffusion enhancing mechanisms, such as submersion in liquids at high temperature.

The primary mechanism of liquid movement into and through intact corn internodes appears to be by bulk transport of liquid, which occurs as the air entrained within cells gets displaced by liquid. Similar fluid penetration mechanisms have previously been hypothesized for penetration of chemicals into wood during wood pulping operations *(5)* and removal of air has been accomplished by "penetration aid" techniques, such as presteaming,

purging, and evacuation. Our method of preheating the segments before impregnation by immersion is similar to the common practice of presteaming of woodchips before liquor impregnation during the paper pulping process. Elevated temperature causes entrained air to expand, driving the air out and reducing the pressure within the void space. When heated segments are submerged in dye solution, the pressure differential generated by the contracting air acts to quickly draw liquid into the void space *(5)*. Under these conditions, cross-sectional segments distal to the internode ends showed the presence of dye in the apoplast surrounding the vascular bundles, but the lack of dye inside the vascular tissue suggests that dye movement occurs directly through the apoplast, specifically along the exterior of the vascular bundles. A proposed mechanism for this result lies in the differential contraction of vascular tissue and parenchyma cells during senescence and drying. As the parenchyma cells contract to a higher extent than vascular tissue (presumably owing to the much higher structural strength of vascular tissue), fissures and cracks are generated along the parenchyma-vascular bundle interface. This structural gap could allow much more rapid and extensive transport of liquids by capillary action, as the gap lacks the physical barriers present in vascular tissue, such as perforation and sieve plates. In addition, because this gap occurs at the parenchyma-vascular bundle interface, the liquid has direct access to the apoplastic continuum, without needing to rely on dye transport out of the vascular bundles and into the apoplast.

Dye transport was slow and uniform distribution was difficult to achieve when impregnation was conducted at atmospheric pressure. Quick and uniform distribution of dye was easily achieved when internodes were preheated before impregnation or impregnated under high vacuum. In both cases, uniform distribution throughout most of the observed pathways mentioned above occurred when the internode void space was 25–35% saturated. Presumably, the remainder of unsaturated volume was the interior void space of the bulk of the parenchyma cells. We speculate that dye may move to the interior of cells immediately surrounding the vascular bundles, but have questioned whether transport occurs into the middle lamella and cell wall layers when the apoplast is fully saturated. If catalyst from the apoplast can be absorbed into the cell walls, then catalyst could be in contact with each hydrolyzable site without the need to saturate the entire parenchyma intracellular space. Complete impregnation of cell walls with catalyst could be achieved with a moisture content of only approx 30%. If our speculations are correct, then one could theoretically achieve catalyst contact with 100% of the cell wall surfaces by saturating only 30% of the internode void volume. This could, in turn, increase the solids content in pretreatment reactors up to about 70%, significantly higher than current solid loadings of about 30–50% *(9,17)*. Higher solids content during pretreatment would result in lower use of process water, reduction in volume of catalyst,

and higher sugar concentrations; all of which would reduce downstream processing costs.

Conclusions

The primary observed pathways for dye transport through our corn internode models were:

1. through the vascular bundles,
2. along the vascular bundle–parenchyma cell interface,
3. throughout the apoplastic continuum, and
4. along the rind–parenchyma interface.

Transport via all routes was initiated at the open ends of the internodes, whereas virtually no transport occurred through the impermeable rind exterior. Air trapped inside cells, particularly the parenchyma, proved to be a difficult barrier, blocking access to the interior cell wall surfaces. Dye transport was slow and a uniform distribution was difficult to achieve when impregnation was conducted at atmospheric pressure. Quick and uniform distribution of dye was achieved when internodes were preheated before impregnation or impregnated under high vacuum. In both cases uniform distribution throughout most of the observed impregnation pathways mentioned above occurred when the internode void space was 25–35% saturated. We speculated that dye may move to the interior of cells surrounding the vascular bundles through pit membranes and question whether transport occurs into the middle lamella when the apoplast is fully saturated. Currently, more experimental work is necessary to bring light to these issues, but if our speculations are correct then one could theoretically achieve catalyst contact with 100% of the cell wall biomass by saturating only 30% of the internode void volume.

In continuation of this work, we will extend our simple internode model studies to include more complex anatomical structures, such as the nodes, and employ higher magnification microscopy tools, such as SEM, TEM, and AFM. We have also initiated experiments aimed at determining how effectively whole internode segments can be pretreated with varying levels of substrate impregnation. Besides providing us with information about catalyst transport in bulk corn stover, this work will also enhance experimental effort to understand interactions occurring in biomass at the ultrastructural and molecular level during both pretreatment and enzymatic hydrolysis.

Acknowledgments

This work was supported by the US Department of Energy (DOE), Office of the Biomass Program. The authors would like to thank Donald Gustafson for supplying the stover used in this study, and Stephanie

Porter, Steven Thomas and Rick Elander for their advice and assistance during preparation of this article.

References

1 Thomas, S., Porter, S., Jurich, J., et al. (2004), *Technical Report FY04-561,* National Renewable Energy Laboratory, Golden, CO.
2 McMillan, J. D. (1994), *ACS Symposium Series* **566,** 292–324.
3 Kazi, K. M. F., Jollez, P., and Chornet, E. (1998), *Biomass Bioenergy* **15,** 125–141.
4 Ramos, L. P. (2003), *Quimica Nova* **26,** 863–871.
5 Malkov, S., Tikka, P., and Gullichsen, J. (2001), *Paper Timber* **83,** 468–473.
6 Esteghlalian, A., Hashimoto, A. G., Fenske, J. J., and Penner, M. H. (1997), *Biores. Technol.* **59,** 129–136.
7 Soderstrom, J., Pilcher, L., Galbe, M., and Zacchi, G. (2003), *Biomass and Bioenergy* **24,** 475–486.
8 Zhu, Y., Lee, Y. Y., and Elander, R. T. (2004), *Appl. Biochem. Biotechnol.* **117,** 103–114
9 Schell, D. J., Farmer, J., Newman, M., and McMillan, J. D. (2003), *Appl. Biochem Biotechnol.* **105/108,** 69–85.
10 Aden, A., Ruth, M., Ibsen, K., et al. (2002), *Technical Report NREL/TP-510-32438,* National Renewable Energy Laboratory, Golden, CO.
11 Kim, K. H., Tucker, M. P., and Nguyen, Q. A. (2002), *Biotechnol. Prog.* **18,** 489–494.
12 Decker, S. and Vinzant, T. (2004), *Office of Biomass Program E Milestone,* ID No. FY04-602.
13 Raven, P. H., Evert, R. F., and Eichhorn, S. E. (1992), *Biology of Plants, 5th edition,* Worth Publishers, Inc., New York.
14 Horobin, R. W. and Kiernan, J. A. (2002), *Conn's Biological Stains,* 10th edition, Biological Stain Commission, Oxford.
15 Mani, S., Tabil, L. G., and Sokhansanj, S. (2004), *Canadian Biosys. Eng.* **46,** 55–61.
16 Kim, S. B. and Lee, Y. Y. (2002), *Biores. Technol.* **83,** 165–171.
17 Tucker, M. P., Kim, K. H., Newman, M. M., and Nguyen, Q. A. (2003), *Appl. Biochem. Biotechnol.* **105,** 165–177.